DOI: 10.1021/ma902252y

Macromolecules
ARTICLE

Analysis of Molecular Aggregation Structures of Fully Aromatic and Semialiphatic Polyimide Films with Synchrotron Grazing Incidence Wide-Angle X-ray Scattering

Junji Wakita,[†] Sangwoo Jin,[‡] Tae Joo Shin,[§] Moonhor Ree,*[,‡] and Shinji Ando*[,†]

[†]*Department of Chemistry and Materials Science, Tokyo Institute of Technology, Ookayama, Meguro-ku, Tokyo 152-8552, Japan,* [‡]*Department of Chemistry, Pohang University of Science & Technology, Pohang 790-784, Korea, and* [§]*Pohang Accelerator Laboratory, Pohang University of Science & Technology, Pohang 790-784, Korea*

Received October 10, 2009; Revised Manuscript Received January 11, 2010

ABSTRACT: The intermolecular aggregation structures of fully aromatic polyimides (Ar-PIs) prepared from pyromillitic dianhydride (PMDA) and those of semialiphatic polyimides (Al-PIs) from 4,4′-diaminocyclohexylmethane (DCHM) were characterized by a grazing incidence wide-angle X-ray scattering (GIWAXS) technique. The aggregation structures of both Ar- and Al-PI thin films formed on Si substrates were identified as a mixture of a liquid-crystalline-like ordered domain and an amorphous matrix. For Ar-PIs whose glass transition temperatures (T_g) are higher than the imidization temperature (T_i), the aggregation structures are significantly influenced by the three-dimensional structures of the PI chain. Rodlike molecular structures with high planarity are prerequisites for the growth of ordered domains of Ar-PIs, whereas an Ar-PI having a bent and nonplanar structure displays the highest intensities of an amorphous halo. In addition, the bulky $-CF_3$ groups in the diamine moiety increase the interchain distance in the ordered domains. On the other hand, for Al-PIs whose T_gs are lower than T_i, the degrees of interchain ordering in the ordered domains were higher than those of Ar-PIs, but the orientation of the ordered domains was decreased significantly by decreasing their T_gs. This is due to the vigorous motion of PI chains during thermal imidization.

1. Introduction

Fully aromatic polyimides (Ar-PI) are well-known high-performance engineering plastics exhibiting outstanding physical and chemical properties: thermal and chemical stability, flame resistance, radiation resistance, mechanical strength, and flexibility.[1] A PI synthesized from pyromellitic dianhydride and bis(4-aminophenyl) ether (PMDA/ODA) and one from 3,3′,4,4′-biphenyltetracarboxylic dianhydride and *p*-phenylenediamine (*s*-BPDA/PDA) are representative ones, and they are known as Kapton-H and Upilex-S, respectively. Ar-PIs have been used in a wide range of high-tech fields, such as aerospace, electric, electronic, and photonic applications. Recently, fluorinated PIs and/or semialiphatic PIs (Al-PIs) have attracted much interest as a new class of electronic and optical material due to their colorlessness, high transparency, low refractive indices, and low birefringence.[2−9] For example, they have been applied to waveguides and optical peripheral components with highly controlled properties in the visible and near-IR regions.[5]

The aggregation structures and the orientation of PI chains in solid films have been investigated because they significantly influence the various properties of PI thin films, such as their thermal, mechanical, and optical properties. For example, PI films having a high orientation on in-plane direction exhibit extraordinarily large in-plane/out-of-plane birefringence[10] and anisotropic thermal expansion.[11] Hasegawa and co-workers[12] proposed a mechanism for spontaneous in-plane orientation during thermal imidization via UV/vis and infrared (IR) dichroic spectra, in which a liquid-crystalline-like highly oriented domain was formed. The in-plane orientation of the domain was developed by the tensile stress induced by the mismatch of thermal expansion between the PI films and the substrates. The present authors have quantitatively estimated the orientation of PI chains in spin-coated films on Si substrates using polarized attenuated total reflection (ATR)/Fourier transform infrared (FT-IR) spectroscopy.[13] PIs having rigid and planar molecular structures exhibited higher degrees of in-plane orientation than those having bent and three-dimensional molecular structures, which is due to decreases in the intermolecular interaction, resulting in a smaller degree of spontaneous chain orientation. These spectroscopic methods can provide averaged structure and property values in films, but it is difficult to separate structural information from the ordered domains and amorphous matrices.

X-ray scattering measurement is a powerful way to distinguish an ordered domain from an amorphous matrix in solid polymers. Quite a few studies have been done on conventional X-ray scattering of various kinds of Ar-PIs.[14−26] For instance, PMDA/ODA films exhibited a variety of aggregation structures, such as amorphous, liquid-crystalline-like, and ordered crystalline structures, depending on the film preparation conditions.[15,22] The aggregation structure of PI chains are schematically illustrated in Figure 1.[22] A PI chain is depicted as a strip with a rectangular cross section owing to the planar chain conformation with benzene rings. The dianhydride and diamine moieties are colored in gray and white on the strip, and the horizontal and vertical directions are parallel and perpendicular to the film surface, respectively. In the crystalline structure (Figure 1a), the PI chains are packed without disorders in the interchain packing, in which the electron-accepting dianhydride and electron-donating diamine

*Corresponding authors: e-mail sando@polymer.titech.ac.jp, tel +81-3-5734-2137, fax +81-3-5734-2889 (S.A.); e-mail ree@postech.edu, tel +82-54-279-2120, fax +82-54-279-3399 (M.R.).

 Published on Web 01/27/2010

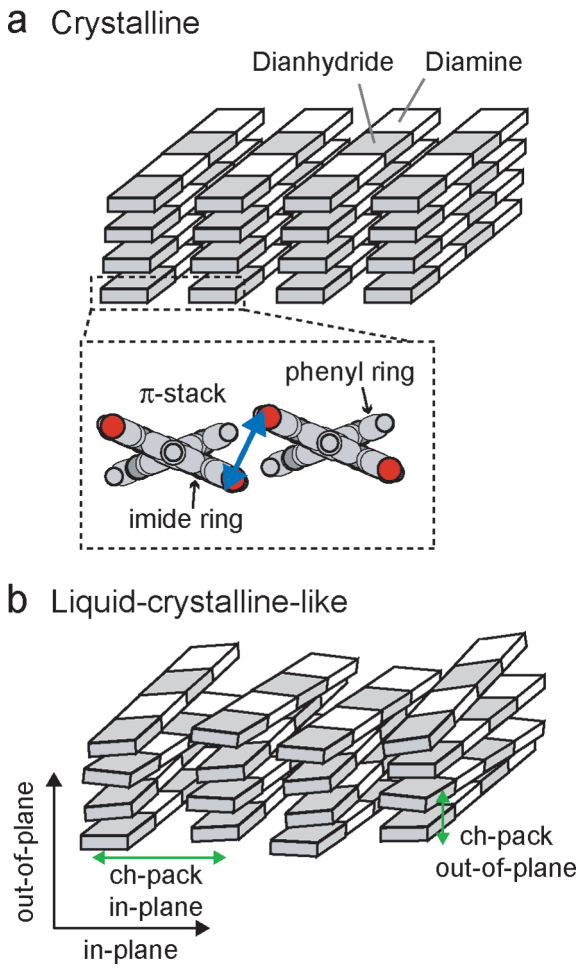

Figure 1. Schematic representation of aggregation structures of PI chains in (a) crystalline and (b) liquid-crystalline-like domain.

moieties of the PI chains are individually stacked, and the structure is known as "preferred layer packing" (PLP)[17] (Figure 2a). In addition, the face-to-face π-stacking of imide and phenyl planar groups between neighboring PI chains is included in the crystalline structure. In the case of poly(4,4′-diphenylene pyromellitimide) (PMDA/BZ) crystallites, of which the unit cell is orthorhombic with a space group symmetry *Pbam*, the (110) and (210) scattering peaks correspond to interchain packing and π-stacking, and their *d*-spacings were reported as 4.66 and 3.39 Å, respectively.[19,20] In contrast, the packing of PI chains is relatively disordered in a liquid-crystalline-like ordered structure due to variation in conformation around the chain axis and the distribution of interchain distances (Figure 1b), though the PI chains have PLP and are packed together both along the in-plane and out-of-plane directions. Accordingly, adjacent stacking between electron-donating diamine moieties and electron-accepting dianhydride moieties, whose structure is known as "mixed layer packing" (MLP)[17] (Figure 2b), is not observed in either the crystalline or liquid-crystalline-like structure. Thereby, the formation of intermolecular charge transfer (CT) complexes between the dianhydride and diamine moieties is highly expected in the amorphous domain in which PI chains are randomly packed.[17] Russell et al.[14] estimated the orientation function by direct measurement of the integrated intensity of reflection peaks in an edge-view pattern. Ree et al.[21,23] reported that Ar-PI chains, which are oriented in the film plane, are more densely packed in the direction of film thickness rather than in the film plane. In general, PI films do not exhibit definitive crystalline scattering peaks, which indicates the absence of large domains with three-dimensional positional order. Such domains

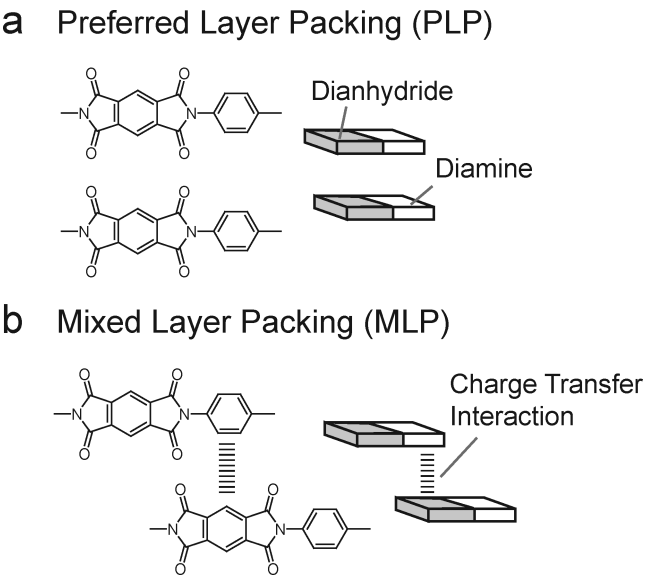

Figure 2. Schematic representation of (a) PLP and (b) MLP structures.

having mesomorphic ordering between the crystalline and amorphous phases can be interpreted as liquid-crystalline-like ordered domains. However, the aggregation structure of PI films at the polymer chain level has not been completely understood yet. First, to our knowledge, the scattering peaks of interchain packing in liquid-crystalline-like ordered domains are not reported even though the presence of such ordered domains was suggested. The broad components at around 15° both in reflection and transmission X-ray scattering patterns were assigned to an amorphous halo, which provides averaged chain distances.[21,23] Second, it is not easy to analyze the structural anisotropy in PI films only from one-dimensional (1D) X-ray scattering patterns. The 1D X-ray scattering only informs a structural characteristic to scanned direction. Hence, if PI chains in ordered domains have different packing order for *x*, *y*, and *z* direction on the film, it is difficult to obtain structural information for the *x*, *y*, and *z* direction at once by using 1D X-ray scattering. Third, to the best of our knowledge, X-ray scattering measurements have not been applied to characterize the Al-PIs derived from alicyclic diamines, and hence their aggregation structures, such as degree of crystallization, orientational order of PI chains, and averaged interchain distance, have not been investigated yet.

For a better understanding of the aggregation structure of PIs, two-dimensional (2D) grazing incidence X-ray scattering (GIXS) measurement should be beneficial because the scatterings in the in-plane and out-of-plane directions can be simultaneously monitored. Recently, this technique has been applied to characterize the aggregation structures of polymer thin films, such as block copolymers,[27−31] polythiophene,[32−35] polyethylene,[36] polyfluorene,[37−39] poly(ethylene terephthalate),[40] poly(trimethylene 2,6-naphthalate),[41] and poly(phenylenevinylene) derivatives.[42,43] Ree and co-workers[27−32] have been clarifying the microphase-separated structure and/or phase transition behavior of various block copolymers formed on Si substrates by quantitative analysis of 2D GIXS patterns. Joshi and co-workers[35] have investigated the thickness dependence of the structural order of poly(3-hexylthiophene). They found that the X-ray scattering profiles displayed Bragg peaks of nanocrystallites diluted in an amorphous matrix, where the orientational distribution of the crystallites changes significantly as a function of film thickness. However, there are a few reports on the GIXS measurements of PI films.[44−47] Factor and co-workers[44] have analyzed the aggregation structure of PMDA/ODA by 1D GIXS measurements. In this paper, the aggregation structures of Ar-PIs and Al-PIs formed on Si substrates will be characterized and

Chart 1. Structures of Polyimides (PIs)

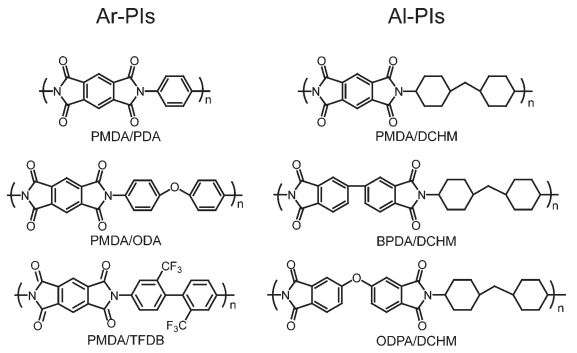

discussed based on the 2D grazing incidence wide-angle X-ray scattering (GIWAXS) technique to clarify the nature and the influence of molecular structures on the aggregation structures of PIs.

2. Experimental Section

2.1. Materials. Pyromellitic dianhydride (PMDA), purchased from Kanto Chemical Co. Inc., was dried at 110 °C and purified by sublimation under reduced pressure. 3,3′,4,4′-Biphenyltetracarboxylic dianhydride (BPDA), purchased from Wako Pure Chemical Industries Ltd., was dried at 170 °C for 12 h under reduced pressure. 4,4′-Oxydiphthalic dianhydride (ODPA), supplied by Shanghai Institute of Synthetic Resins, was dried at 150 °C for 12 h under reduced pressure. 4,4-Diaminodiphenyl ether (ODA), purchased from Wako Pure Chemical Industries Ltd., was recrystallized from tetrahydrofuran, followed by sublimation under reduced pressure. 2,2′-Bis(trifluoromethyl)-4,4′-diaminobiphenyldiamine (TFDB), supplied by Central Glass Co. Ltd., was used as received. 4,4′-Diaminocyclohexylmethane (DCHM), purchased from Tokyo Kasei Kogyo Co. Ltd., was recrystallized from *n*-hexane and sublimed under reduced pressure. *N,O*-Bis(trimethylsilyl)trifluoroacetamide (99+%, BSTFA) and *N,N*-dimethylacetamide (anhydrous, DMAc), purchased from Aldrich, were used without further purification.

2.2. Preparation of Polyimide Films. The molecular structures of PIs used in this study are shown in Chart 1. The precursors of Ar-PIs, poly(amic acid)s (PAAs), were prepared by mixing equimolar amounts of dianhydride and diamine dissolved in DMAc under a dried nitrogen atmosphere. The PAA solutions were stirred at room temperature for 48 h. The precursors of Al-PIs, poly(amic acid) silyl ester (PASE), were prepared by the *in situ* silylation method reported by Matsumoto[48] and Oishi.[49,50] For instance, DCHM was dissolved in DMAc and stirred for a few minutes, and then a 1.05 molar amount of BSTFA was slowly added. An equimolar amount of dianhydride was then added and stirred at room temperature for 48 h to give a PASE solution. The trimethylsilylation of the amino groups of diamines by BSTFA can avoid salt formation between unreacted amino and carboxyl groups. In general, PAA and PASE solutions become viscous after stirring for several hours depending on the degree of polymerization and the rigidity of the molecular structures. Furthermore, a previously prepared 10 wt % NMP solution of PMDA/PDA PAA was also used. PI films were successively prepared by thermal imidization of the corresponding precursors. The PAA and PASE solutions were spin-coated onto Si substrates, followed by soft baking at 70 °C for 1 h and subsequent thermal imidization at 300 °C for 1.5 h on a hot plate at a ramping rate of 10 °C/min. All curing procedures were conducted under nitrogen flow.

2.3. Measurement. Thermomechanical analysis (TMA) was conducted with a Shimadzu TMA-60 with a fixed load of 3.0 g and a heating rate of 5 °C/min. The glass transition temperatures (T_g) were estimated by the point where two tangent lines drawn on the curve intersect.[51] The film thicknesses of the PI films were measured with a probe-pin type surface profilometer (DEKTAK-III).

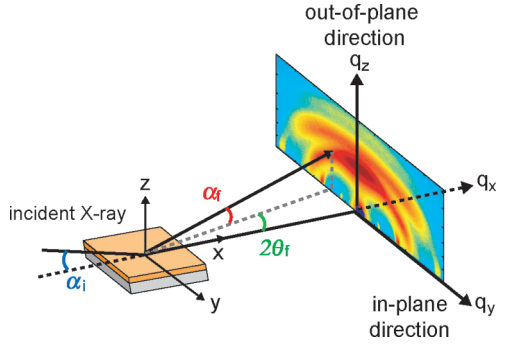

Figure 3. GIWAXS geometry: α_i is the incident angle at which the X-ray beam impinges on the film surface; α_f and $2\theta_f$ are the exit angles of the X-ray beam with respect to the film surface and to the plane of incidence, respectively, and q_x, q_y, and q_z are the components of the scattering vector, **q**.

GIWAXS measurements (Figure 3) were carried out at the 4C2 beamlines[52−54] at the Pohang Accelerator Laboratory. A monochromatized X-ray radiation source of 8.05 keV (λ = 0.138 nm: λ, wavelength) and a two-dimensional charge-coupled device (2D CCD) detector (Roper Scientific, Trenton, NJ) were used. The sample-to-detector distance was 127.6 and 133.9 mm. A set of aluminum foil strips was employed as semitransparent beam stops because the intensity of the specular reflection from the substrate is much stronger than the intensity of GIWAXS near the critical angle. Samples were mounted on a homemade *z*-axis goniometer equipped with a vacuum chamber. α_f and $2\theta_f$ are the exit angles of the X-ray beam with respect to the film surface and to the plane of incidence. The incidence angle α_i of X-ray beam was set in the range 0.16°−0.20°, which is between the critical angles of the PI polymer films[44] and the silicon substrate ($\alpha_{c,f}$ and $\alpha_{c,s}$). Scattering angles were corrected by the positions of X-ray beams reflected from the silicon substrate interface with changing incidence angle α_i and by a precalibrated silver behenate (TIC, Japan). Data were typically collected for 30 s.

2.4. Quantum Chemical Calculation. The density functional theory (DFT) with a three-parameter Becke-style hybrid functional (B3LYP)[55−57] with 6-311G(d) basis set was adopted for obtaining the optimized structure of PI model compounds. All calculations were performed with a Gaussian-03 D.02[58] program package installed in the Global Scientific Information and Computing Center (GSIC), Tokyo Institute of Technology.

3. Results and Discussion

3.1. Fully Aromatic PMDA-PIs. Figure 4 shows the representative 2D GIWAXS patterns of (a) PMDA/PDA (thickness: 4.9 μm), (b) PMDA/ODA (6.2 μm), and (c) PMDA/TFDB (8.3 μm) PI films. The out-of-plane and in-plane 1D GIWAXS profiles extracted along the α_f direction at $2\theta_f$ = 0° and $2\theta_f$ direction at α_f = 1.03° from the 2D GIWAXS patterns are shown in parts a and b of Figure 5, respectively. The scattering profiles extracted with azimuthal angle (μ) at the peak positions in the out-of-plane profiles (Figure 5a, (a) α_f = 17.2°, (b) 15.8°, and (c) 14.3°) (azimuthal profile) are shown in Figure 5c. The out-of-plane and in-plane profiles of PMDA-PIs were fitted with Gaussian broadening functions to estimate the central peak positions. Thin solid and dotted lines represent the scattering peaks from the ordered domains and the amorphous matrix, respectively. The peak positions, the calculated *d*-spacings, and the assignment of peaks obtained by peak fitting with Gaussian broadening functions are listed in Table 1. The calculated *d*-spacing of each peak is abbreviated as *d* ("assignment").

The 2D GIWAXS pattern of PMDA/PDA film shows an isotropic scattering ring at around 16° and intense scattering arcs at around 17° and 22° along the out-of-plane direction

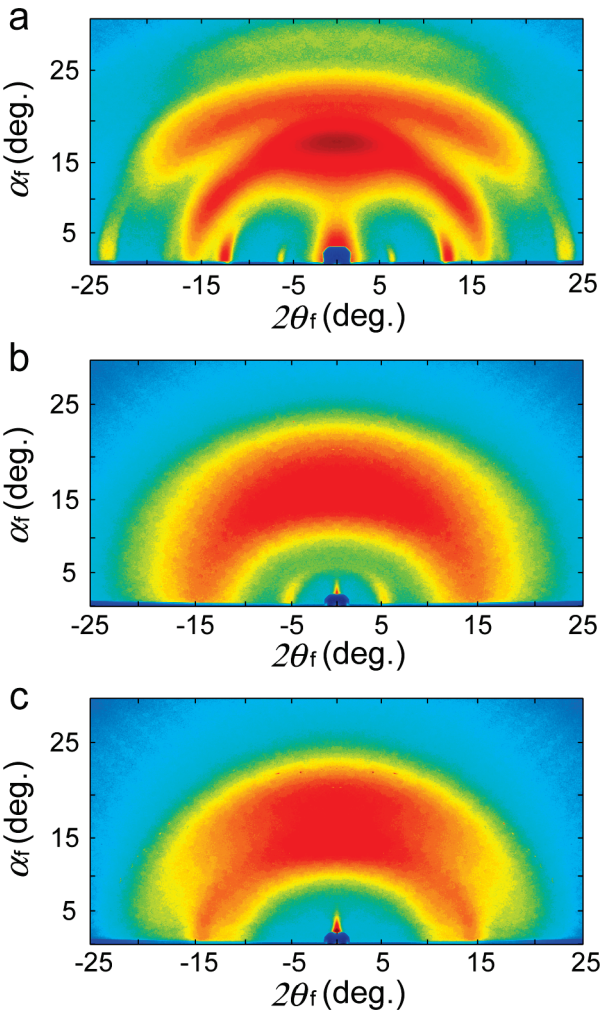

Figure 4. 2D GIWAXS patterns of (a) PMDA/PDA, (b) PMDA/ODA, and (c) PMDA/TFDB thin films prepared on silicon substrates.

(Figure 4a). Here, the isotropic scattering ring is assignable to an amorphous halo,[59] and hence the scattering arcs originate from an ordered structure. From the peak fitting of the out-of-plane profile (Figure 5a), the scattering peak originating from the ordered domains are observed at 17.05° and 22.08°, respectively. The azimuthal profile at the former peak position (Figure 5c) showed maximum intensity at $\mu = 90°$, which means that the ordered structure is oriented normal to the film plane. In addition, the calculated *d*-spacing (4.66 Å) agrees well with the typical value of interchain distances of PMDA/PDA (4.70 Å).[21] Accordingly, the scattering arc at around 17° in the 2D patterns originates from the packing of PI chains normal to the film plane in the ordered domains. Hereafter, this kind of packing structure of PI chains will be abbreviated as "ch-pack". If PI chains are well packed with a higher order in the interchain

Table 1. Peak Positions, *d*-Spacings, and Assignment of Fully Aromatic PMDA-PIs

	peak position (deg)	*d*-spacing (Å)	assignment
PMDA/PDA out-of-plane	17.05	4.66	ch-pack
	22.08	3.61	π-stack
	15.94	4.98	amorphous halo
PMDA/PDA in-plane	6.46	12.25	(001)
	12.63	6.27	(002)
	16.16	4.91	ch-pack
	18.11	4.38	(003)
	23.12	3.44	(004)
	14.52	5.46	amorphous halo
PMDA/ODA out-of-plane	15.26	5.19	ch-pack
	20.29	3.92	π-stack
	16.00	4.96	amorphous halo
PMDA/ODA in-plane	5.24	15.10	(002)
	14.70	5.40	ch-pack
	14.11	5.60	amorphous halo
PMDA/TFDB out-of-plane	13.99	5.67	ch-pack
	19.90	3.99	π-stack
	16.07	4.94	amorphous halo
PMDA/TFDB in-plane	11.82	6.71	ch-pack
	14.39	5.51	(003)
	13.69	5.79	amorphous halo

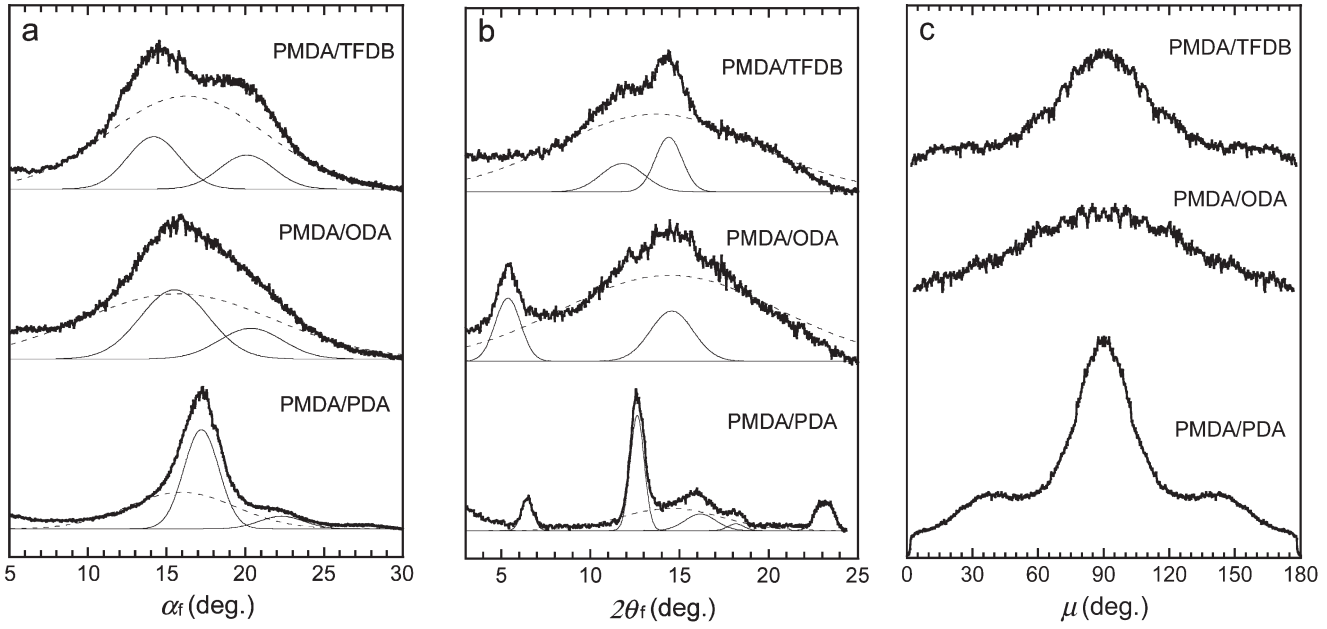

Figure 5. GIWAXS profiles of Ar-PIs: (a) out-of-plane profiles, (b) in-plane profiles, and (c) azimuthal profiles at the ch-pack peak position. Thin solid and dotted lines represent the scattering peaks from the ordered domains and the amorphous matrix, respectively.

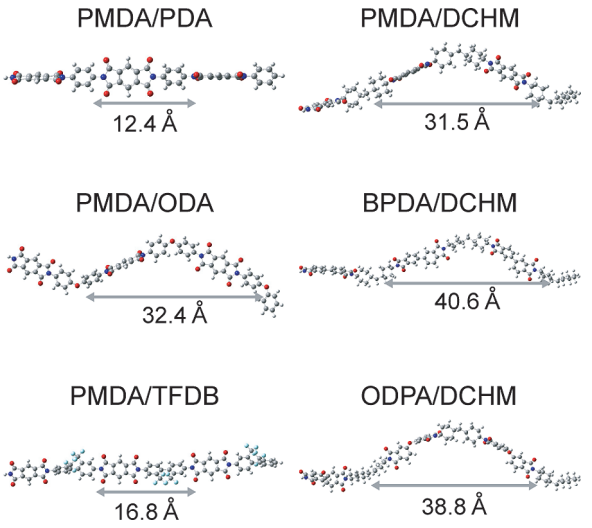

Figure 6. Optimized structures of PI trimer models obtained by DFT calculations at the level of B3LYP/6-311G(d).

packing as in the crystalline state, the ch-pack peak should split into several sharp peaks. This is the case with BPDA/PDA PI film,[21] in which sharp peaks assignable to (110) and (200) scatterings were clearly observed in the reflection X-ray pattern. The absence of splits on the ch-pack peak at 17.05° in the out-of-plane profile (Figure 5a) indicates that the structures of PI chain packing included in the ordered domains can be interpreted as liquid-crystalline-like structures, as shown in Figure 1b. The positional order of PI chains along the out-of-plane direction could be disturbed by variation in the conformations around the chain axis and distribution of the interchain distances. In contrast, the calculated *d*-spacing of the latter scattering at 22.08° (3.61 Å) is smaller than that of the ch-pack (4.66 Å) but close to the *d*-spacing of the (210) plane of a highly crystalline PMDA/BZ PI (3.39 Å), as noted in the Introduction.[19,20] Therefore, the scattering at 22.08° could be assignable to the $\pi-\pi$ stacking of imide and phenyl rings in the ordered domains (Figure 1a). Hereafter, this kind of stacking structure will be abbreviated as "π-stack". On the other hand, several scattering arcs appear at around 6°, 12°, 18°, and 23° along the in-plane direction in the 2D GIWAXS pattern, whose relative scattering vector lengths estimated from the specular reflection positions are 1, 2, 3, and 4, respectively (Figures 4a and 5b). According to the transmission X-ray pattern of PMDA/PDA film,[21] they are attributable to the scattering of (001), (002), (003), and (004) planes along the PI chain axis. As seen in the pattern, the intensity of (002) peak is significantly higher than those of other (00*l*) peaks. The scattering intensity is influenced by the form factor which describes the shapes, sizes, and orientations of scatters. Hence, the scattering peaks can appear or disappear, and further the intensity of scattering peak can be enhanced or reduced due to specific molecular structure and packing geometry.[59] Accordingly, the highest intensity of the (002) peak is ascribable to the influence of form factor. The periodic length along the PI chain (*L*) in the ordered domains was estimated to be 12.25 Å for PMDA/PDA. Figure 6 depicts the optimized molecular structures of the trimer models of PIs. The *L* value coincides with the calculated length of a repeating unit (12.4 Å shown in Figure 6), which reveals that one repeating unit corresponds to the periodic structure along the PI chains. In the case of poly(ethylene terephthalate) (PET) film, the (00*l*) peaks were not observed in the amorphous matrix, but they were observed in the liquid crystalline phase, in which neighboring repeating units of PET chains are

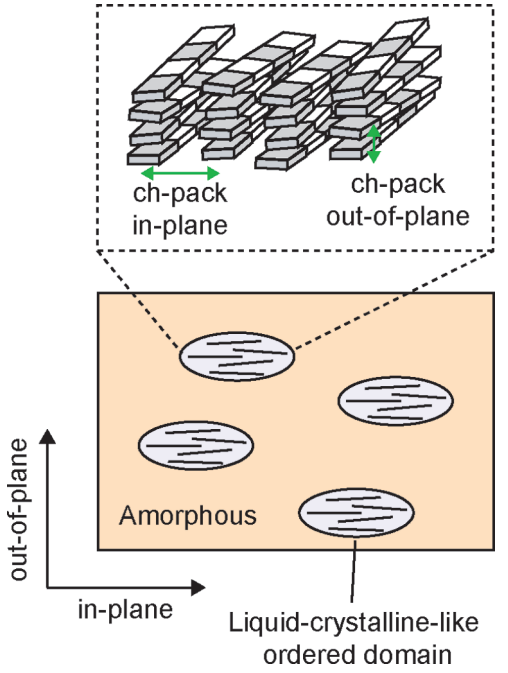

Figure 7. Schematic illustration of aggregation structure of Ar-PIs. Lines correspond to the PI chains, and circles denote the liquid-crystalline-like ordered domains.

laterally ordered.[60] On analogy with the case of PET film, the (00*l*) peaks observed for PMDA/PDA originates from the liquid-crystalline-like ordered domains, in which the alternating dianhydride and diamine moieties are laterally stacked along the in-plane direction (the PLP structure shown in Figures 1b and 2a). Thereby, the peak observed at around 16.16° in the in-plane profile (Figure 5b) represents a ch-pack structure along the in-plane direction in the ordered domains (Figure 1b). Furthermore, the absence of (00*l*) peaks in the out-of-plane profile (Figure 5a) indicates that the PI chains included in the ordered domains are preferentially oriented parallel to the film plane. Meanwhile, the broad peak centered at 14.52° which overlaps with the scattering peaks of (002), (003), and ch-pack is attributable to an amorphous halo (Figure 5b). On the basis of these results, the aggregation structure of PI chains in PMDA/PDA film can be interpreted as a mixture of amorphous matrix and liquid-crystalline-like ordered domains, in which long-range three-dimensional positional order is absent. The schematic illustration for the aggregation structure is shown in Figure 7. The solid lines represent rigid-rod PI chains, and the elliptic circles denote liquid-crystalline-like ordered domains. The molecular axes of the PI chains in the ordered domains are preferentially oriented parallel to the film plane and packed together in the PLP structure (Figure 2a) along both the in-plane and the out-of-plane directions. In other words, the directors of the liquid-crystalline-like ordered domains are preferentially oriented in the film plane.

The 2D GIWAXS pattern of PMDA/ODA film shows a broad isotropic scattering ring of amorphous halo (Figure 4b). However, peak fitting of the out-of-plane profile revealed that two weak scattering peaks at 15.26° and 20.29° overlap on an amorphous halo (Figures 5a). The former peak is not split into several peaks, and the azimuthal profile at the peak position shows the maximum intensity at $\mu = 90°$ (Figure 5c). These features are similar to those of PMDA/PDA film, and therefore the peak at 15.26° is assignable to the scattering peaks of ch-pack included in the liquid-crystalline-like domains in which PI chains are packed normal to the film plane.

Further, the latter peak at 20.29° is assignable to the π-stack of the imide and phenyl rings on analogy with PMDA/PDA (Figure 5a). In the in-plane profile, sharp and broad scattering peaks were respectively observed at around 5° and 15° (Figures 4b and 5b). According to the literature,[14−16,22,44,46] the former peak is assignable to the scattering of (002) plane of periodicity along the PI chains, indicating that PI chains are laterally packed along the in-plane direction in ordered domains. As depicted in Figure 6, the main chain of PMDA/ODA has a bent structure at the diphenyl ether (−O−) linkage, and the calculated length of the two repeating units is 32.4 Å. This value is close to the periodic length along the PI chains estimated from the (002) peak at 5.24° (30.20 Å). Accordingly, a curved structure consisting of two repeating units corresponds to the periodic structure along PI chains in PMDA/ODA film, which agrees with the results of a previous study.[22] Moreover, PI chains are preferentially oriented parallel to the film plane in ordered domains because (00*l*) peaks are absent in the out-of-plane profile. Unlike PMDA/PDA film, however, higher-order (00*l*) peaks were not observed for PMDA/ODA film. This reveals that the interchain ordering along the in-plane direction is not as high as that of PMDA/PDA. This could be induced by the off-planar defects in the packing structure, which may be caused by the twisted conformations around the ether linkages in the diamine moiety of PMDA/ODA. Hence, the scattering from the ch-pack is expected to be weak in the in-plane profile. In fact, the broad scattering peak appearing at around 15° in the in-plane profile is characterized as a weak ch-pack peak at 14.70°, overlapping with a strong and broad amorphous halo centered at 14.11°. On the basis of these results, the aggregation structure of PMDA/ODA is interpreted as a mixture of the amorphous matrix and the liquid-crystalline-like ordered domains which are oriented in the film plane as illustrated in Figure 7. However, the order of the interchain packing is considered to be significantly lower than that of PMDA/PDA.

The 1D and 2D GIWAXS patterns of PMDA/TFDB film (Figures 4c and 5a−c) also indicate that the aggregation structure of PMDA/TFDB film is a mixture of the amorphous matrix and the liquid-crystalline-like ordered domains. In the ordered domains, PI chains are oriented parallel to the film plane and packed together along the in-plane and out-of-plane directions. A broad amorphous halo, a ch-pack peak, and a π-stack peak are observed at around 16°, 14°, and 20° along the out-of-plane direction, respectively. On the other hand, the in-plane profile shows a peak at around 14°, a shoulder peak at around 12°, and a broad amorphous halo at around 13°. According to the literature,[23] the peak at around 14° is assignable to the scattering of (003) plane of periodicity along PI chains in ordered domains. The periodic length along the PI chains estimated for PMDA/TFDB having a rigid-rod molecular structure is 16.53 Å. This value coincides well with the calculated length of one repeating unit (16.7 Å, see Figure 6), which indicates that one repeating unit corresponds to the periodic structure along PI chains. The shoulder peak observed at around 12° is assignable to the ch-pack peak because its position does not match any scattering angles for (00*l*) peaks, in which the scattering angles for the (001) and (002) peaks estimated from that of (003) are 4.79° and 9.60°, respectively. The absence of (001) and (002) peaks in the pattern is also ascribable to the influence of form factor as well as PMDA/PDA.

The value of *d*(ch-pack) apparently reflects the three-dimensional structures of PI chains. The larger *d*(ch-pack) value for PMDA/ODA (5.19 and 5.40 Å) than that for PMDA/PDA (4.66 and 4.91 Å) (Table 1) is attributable to the bent structure of the former PI chains which prevents close chain packing in the ordered domains. In the case of PMDA/TFDB, the *d*(ch-pack) values along the out-of-plane (5.67 Å) and in-plane (6.71 Å) directions are significantly larger than those of the other PMDA−PIs (4.66−5.40 Å). However, the *d*(amorphous) values (4.94 and 5.79 Å) are close to those of the other Ar-PIs (4.96−5.60 Å) (Table 1). This implies that the interchain packing of PMDA/TFDB in the ordered domains could be looser than those of the other Ar-PIs. As mentioned above, the alternating dianhydride and diamine moieties are individually stacked in the ordered domains (PLP structure), which leads to significant steric hindrance between the bulky $-CF_3$ groups of neighboring diamine moieties. This should be the main cause of the increase in the *d*(ch-pack) of PMDA/TFDB. In addition, the *d*(ch-pack) along the in-plane direction (6.71 Å) is particularly larger than that in the out-of-plane direction (5.67 Å). This strongly suggests that the C−C vectors of the $C-CF_3$ side groups are preferentially oriented in the film plane, and it also indicates that the benzene rings in the diamine moieties are preferentially oriented parallel to the film plane. In contrast, the dianhydride and diamine moieties are randomly stacked in the amorphous matrix, which may not induce sterically hindered packing structures among PI chains. This could be one reason why the *d*(amorphous) values of PMDA/TFDB (4.94, 5.79 Å) are close to those of the other Ar-PIs (4.96−5.60 Å).

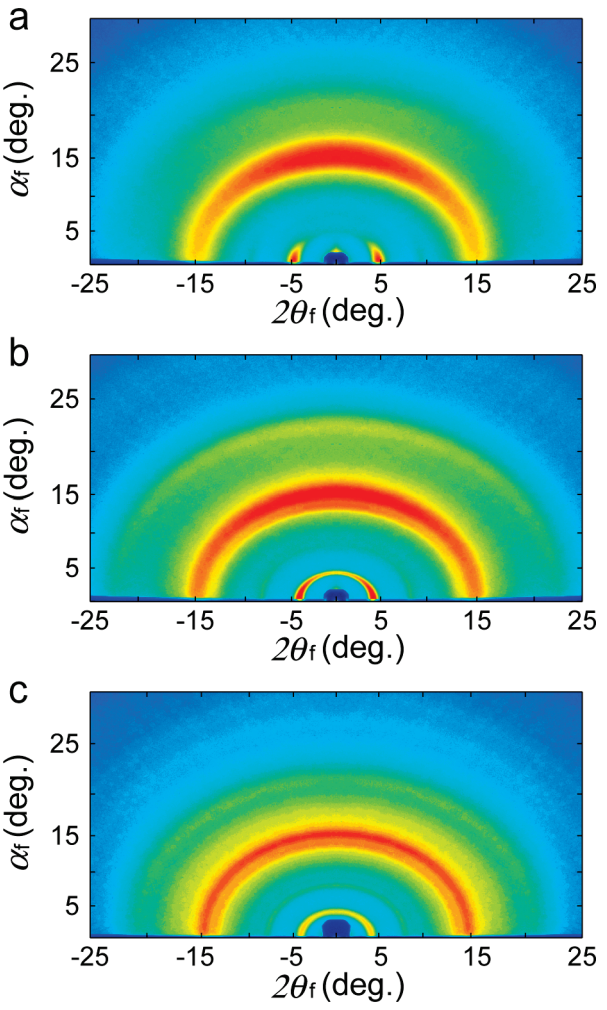

Figure 8. 2D GIWAXS patterns of (a) PMDA/DCHM, (b) BPDA/DCHM, and (c) ODPA/DCHM thin films prepared on silicon substrates.

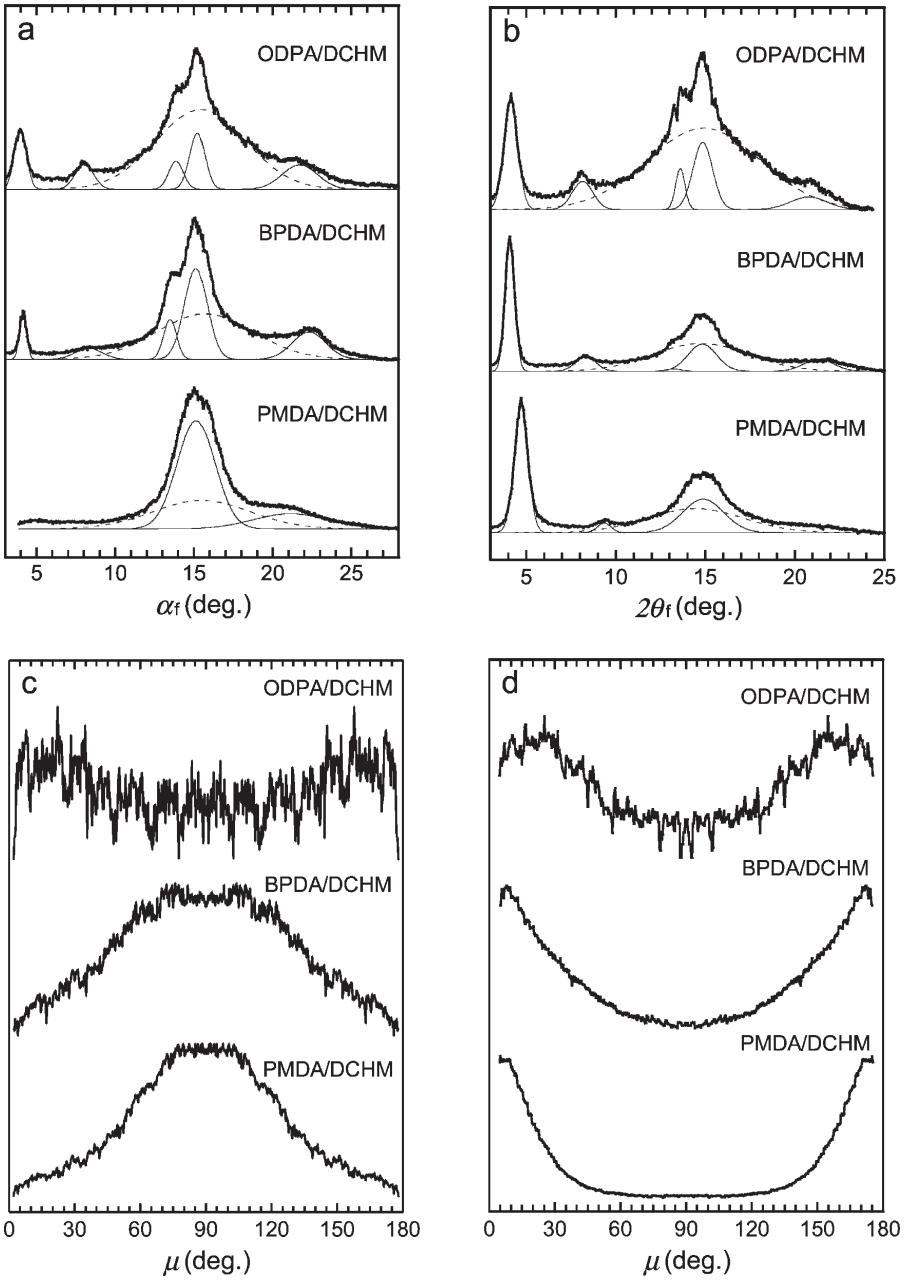

Figure 9. GIWAXS profiles of Al-PIs: (a) out-of-plane profiles, (b) in-plane profiles, and azimuthal profiles at (c) the ch-pack peak position and (d) the (002) peak position. Thin solid and dotted lines represent the scattering peaks from the ordered domains and the amorphous matrix, respectively.

The intensities of the amorphous halos increased in the order of PMDA/PDA < PMDA/TFDB < PMDA/ODA, indicating that the proportion of the amorphous matrix increased in this order. The linear and planar molecular structure of PMDA/PDA (Figure 6) should be favorable for the growth of highly ordered domains. In the case of PMDA/ODA, the bent molecular structure kinked at the diphenyl ether linkage prevents the extensive growth of highly ordered domains. Although PMDA/TFDB possesses a rodlike structure similar to PMDA/PDA (Figure 6), the bulky $-CF_3$ groups at the diamine moiety do not promote the growth of ordered domains. This is supported by the fact that the proportion of amorphous matrix is intermediate between those of the other Ar-PIs. Consequently, a linear and planar molecular structure is required for the extensive growth of highly ordered domains, whereas bent main chain structures and/or bulky side groups prevent the growth of ordered domains.

In addition, both of the *d*(ch-pack) and *d*(amorphous) values along the out-of-plane direction are smaller than those along the in-plane direction, regardless of the steric structure of PI chains (Table 1). This clearly indicates that PI chains are densely packed in the direction of film thickness rather than in the film plane, both in the amorphous matrix and in the liquid-crystalline-like ordered domains, as noted in the literature.[21,23]

3.2. Semialiphatic DCHM-PIs. Figure 8 shows the representative 2D GIWAXS patterns of semialiphatic PMDA/DCHM (thickness: ca. 5.6 μm) (a), BPDA/DCHM (8.7 μm) (b), and ODPA/DCHM (5.2 μm) (c) PI films. The out-of-plane and in-plane GIWAXS profiles extracted along the α_f direction at $2\theta_f = 0°$ and $2\theta_f$ direction at $\alpha_f = 1.03°$ from the 2D GIWAXS patterns are shown in parts a and b of Figures 9, respectively. The azimuthal profiles extracted at the scattering peak position in the out-of-plane profiles

Table 2. Peak Positions, *d*-Spacings, and Assignment of Semialiphatic DCHM-PIs

	peak position (deg)	*d*-spacing (Å)	assignment
PMDA/DCHM out-of-plane	14.89	5.33	ch-pack
	20.97	3.79	π-stack
	15.25	5.20	amorphous halo
PMDA/DCHM in-plane	4.70	16.82	(002)
	9.35	8.47	(004)
	14.88	5.33	ch-pack
	14.43	5.50	amorphous halo
BPDA/DCHM out-of-plane	3.90	20.30	(002)
	8.06	9.81	(004)
	13.24	5.99	ch-pack
	14.87	5.33	ch-pack
	22.06	3.61	π-stack
	15.46	5.13	amorphous halo
BPDA/DCHM in-plane	4.08	19.37	(002)
	8.31	9.52	(004)
	13.22	5.99	ch-pack
	14.77	5.37	ch-pack
	21.34	3.73	π-stack
	14.77	5.37	amorphous halo
ODPA/DCHM out-of-plane	3.85	20.58	(002)
	7.92	10.00	(004)
	13.74	5.77	ch-pack
	15.09	5.26	ch-pack
	21.59	3.69	π-stack
	15.30	5.19	amorphous halo
ODPA/DCHM in-plane	4.14	19.11	(002)
	8.14	9.73	(004)
	13.60	5.83	ch-pack
	14.86	5.34	ch-pack
	20.78	3.83	π-stack
	14.91	5.32	amorphous halo

(Figure 9a, (a) $\alpha_f = 15.0°$, (b) 15.1°, (c) 15.2°) and the in-plane profiles (Figure 9b, (a) $2\theta_f = 4.7°$, (b) 4.1°, (c) 4.1°) are shown in parts c and d of Figure 9, respectively. The out-of-plane and in-plane profiles were fitted with Gaussian broadening functions to estimate the central peak positions. Thin solid and dotted lines represent the scattering peaks originating from the ordered domains and the amorphous matrix, respectively. The peak positions, the calculated *d*-spacings, and the assignment of peaks obtained by peak fitting with Gaussian broadening functions are listed in Table 2.

The 2D GIWAXS pattern of PMDA/DCHM film shows a scattering arc at around 15° along the out-of-plane direction, which is overlapped with the broad isotropic scattering ring assignable to the amorphous halo (Figure 8a). The scattering peak at 14.89° in the out-of-plane profile (Figure 9a) was not split into several sharp peaks, and the azimuthal profile in Figure 9c shows the maximum intensity at $\mu = 90°$. These characteristics are consistent with the other PMDA-PIs described above, and thus the scattering arc should represent the packing of PI chains along the direction normal to the film plane. Such packing structures should be included in the liquid-crystalline-like ordered domains. In addition, another scattering peak was observed at around 20.97° in the out-of-plane profile (Figure 9a). Since the calculated *d*-spacing (3.79 Å) is close to the *d*(π-stack) of Ar-PIs (3.61−3.99 Å) as stated in section 3.1, this peak is assignable to $\pi-\pi$ stacking of imide rings in the ordered domains (Figure 1a). On the other hand, two scattering arcs were observed at around 5° and 9° along the in-plane direction in the 2D pattern, whose relative scattering vector lengths estimated from the specular reflection positions are 1 and 2, respectively (Figures 8a and 9b). As depicted in Figure 6, PMDA/DCHM has a bent molecular structure kinked at the methylene ($-CH_2-$) linkage in the diamine moiety, and the calculated length of the two repeating units is 31.5 Å, of which half the value is close to the *d*-spacing estimated from the scattering peak at 4.70° in the in-plane profile (16.82 Å). On analogy with the case of PMDA/ODA, the scattering arcs are assignable to the scatterings of (002) and (004) planes of periodicity along PI chains in the ordered domains, respectively. This indicates that a curved structure consisting of two repeating units corresponds to the periodic structure along PI chains in PMDA/DCHM film. Moreover, (00*l*) peaks were not observed in the out-of-plane profile. Based on these findings, PI chains are preferentially oriented parallel to the film plane and laterally packed along the in-plane direction in the liquid-crystalline-like ordered domains. Therefore, the sharp scattering peak observed at around 14.88° in the in-plane profile corresponds to the packing of PI chains parallel to the film plane in the ordered domains. Further, a broad component centered at 14.43° which overlaps with the scattering peak of ch-pack in the in-plane profile is attributable to the amorphous halo. Consequently, the aggregation structure of PMDA/DCHM film is interpreted as a mixture of the amorphous matrix and the liquid-crystalline-like ordered domains which are oriented in the film plane.

PMDA/DCHM film exhibits a higher structural order than PMDA/ODA. First, the amorphous halo of PMDA/DCHM is weaker than that of PMDA/ODA, suggesting that the proportion of the amorphous matrix is lower than that of PMDA/ODA (Figures 5 and 9). Second, a higher-order (004) peak was clearly observed for PMDA/DCHM, which indicates that PMDA/DCHM has a higher interchain ordering along the in-plane direction compared with PMDA/ODA (Figures 5b and 9b). However, PMDA/DCHM obviously has a nonplanar and bent molecular structure, which is similar to PMDA/ODA (Figure 6), and hence the high structural order in PMDA/DCHM is not explainable only from the steric effects of the molecular structure. Note that a significant enhancement of interchain ordering could be induced by molecular rearrangement occurring during thermal imidization owing to high chain mobility,[15,18,22] and hence the effects of annealing on the aggregation structure of PIs should be relevant to the glass transition temperature (T_g).[15,18] Takahashi and co-workers[15] have reported that a significant enhancement of interchain ordering along the chain axis begins to occur in PMDA/ODA between 300 and 350 °C. The glass transition of PMDA/ODA starts in this temperature range. Further, Cheng and co-workers[18] reported that the crystallization of BPDA/TFDB PI having a rodlike structure was significantly promoted by thermal treatment over T_g (425 °C). PMDA/DCHM exhibited a relatively low T_g (320 °C) (see the TMA curves in Figure 10) due to the bulky and flexible structure of the DCHM moiety consisting of two cyclohexyl rings and a methylene linkage. This T_g is close to the imidization temperature (T_i: 300 °C), and therefore the molecular rearrangement of PMDA/DCHM during thermal imidization could be more vigorous than that of PMDA/ODA (T_g: 415 °C) (see the TMA curves in Figure 10). The rigid dianhydride moieties of PMDA tend to be stacked together through the dipolar−dipolar interactions between adjacent imide groups, which leads to the PLP structure. The formation of PLP could be promoted by the vigorous rearrangement and translational motion of PI chains at temperatures close to T_g. This should be the main cause of the higher structural order of PMDA/DCHM compared to PMDA/ODA.

The out-of-plane and in-plane profiles of BPDA/DCHM and ODPA/DCHM films (Figure 9a,b and Table 2) show the scattering peaks of (002), (004), ch-pack, π-stack, and an amorphous halo similar to PMDA/DCHM film. This indicates

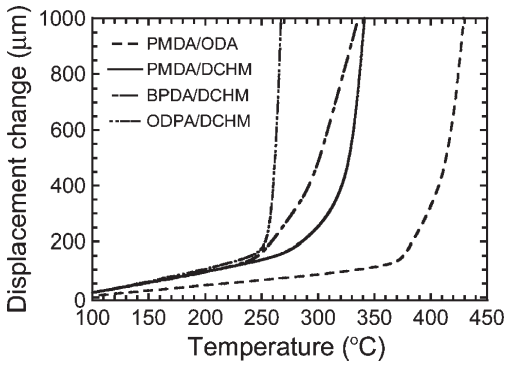

Figure 10. TMA curves of PMDA/ODA, PMDA/DCHM, BPDA/DCHM, and ODPA/DCHM.

that their aggregation structures are also interpreted as a mixture of the amorphous matrix and the liquid-crystalline-like ordered domains.

The orientation of the ordered domains decreased significantly in the order of PMDA/DCHM > BPDA/DCHM > ODPA/DCHM. The 2D GIWAXS pattern of PMDA/DCHM film shows clear scattering arcs for (002) and (004) plane along the in-plane direction, and thus the maximum intensities of the azimuthal profiles at the peak position of (002) are observed at $\mu = 0°$ and 180° (Figure 9d). This indicates that PI chains are preferentially oriented in the film plane. On the other hand, the scattering arcs of BPDA/DCHM broadened to the out-of-plane direction, and finally they merged into the isotropic scattering ring in ODPA/DCHM (Figure 8). Accordingly, ODPA/DCHM exhibits a relatively flat azimuthal profile without sharp and high intensities at $\mu = 0°$ and 180° (Figure 9d), which indicates the lower order of the in-plane orientation of PI chains. This is the reason why the (00*l*) peaks are clearly observed in the out-of-plane profiles of BPDA/DCHM and ODPA/DCHM (Figure 9a). In addition, the scattering arc of ch-pack in the 2D GIWAXS pattern of BPDA/DCHM broadened to the in-plane direction compared with that of PMDA/DCHM, and ODPA/DCHM exhibits a narrow isotropic scattering ring assignable to the ch-pack (Figure 8). The peak maximum of the azimuthal profiles at the peak position of ch-pack is located at around $\mu = 90°$ in PMDA/DCHM film (Figure 9c), which indicates that the packing direction of PI chains in the ordered domains are normal to the film plane. In contrast, ODPA/DCHM exhibits a featureless azimuthal profile without peaks (Figure 9c), which demonstrates that the packing of PI chains in the ordered domains possesses nearly isotropic distribution. On the basis of these results, one can conclude that the directors of the liquid-crystalline-like ordered domains of BPDA/DCHM are tilted with respect to the film surface, and those of ODPA/DCHM are isotropically oriented in the film. This is the reason why the in-plane and out-of-plane profiles of BPDA/DCHM and ODPA/DCHM are similar to each other (Figure 9a,b).

It was reported that the structural transition from the in-plane orientation to the isotropic state is induced by a large-scale translational motion of PI chains in PMDA/ODA film.[22] In comparison, the T_gs of these Al-PIs increased in the order of ODPA/DCHM (258 °C) < BPDA/DCHM (278 °C) < PMDA/DCHM (320 °C) (see the TMA curves in Figure 10). Since the T_gs of the former two PIs are lower than the imidization temperature (300 °C), the translational motion of these PI chains in the amorphous matrix during thermal imidization should be much more vigorous than that of PMDA/DCHM, and this chain motion should disturb the

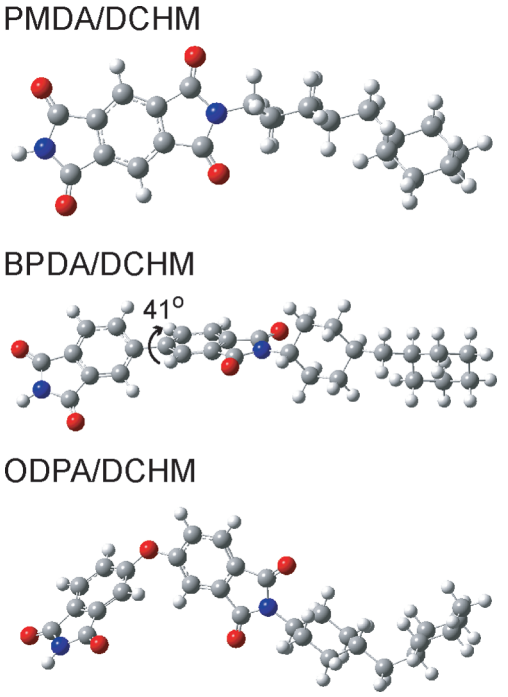

Figure 11. Optimized structures of Al-PI repeating units obtained by DFT calculations at the level of B3LYP/6-311G(d).

in-plane orientation of the ordered domains. The disruption of in-plane orientation in liquid-crystalline-like ordered domains induced by thermal treatment was also observed for poly(2-methoxy-5-(2′-ethylhexyloxy-1,4′-phenylene-vinylene) (MEH-PPV) films.[42] On the other hand, such vigorous motion of these PIs induces more significant molecular rearrangement during thermal imidization compared with PMDA/DCHM, which enhances the interchain ordering of BPDA/DCHM and ODPA/DCHM with bent molecular structures. The ch-pack peak was split into two peaks (BPDA/DCHM: 13.24° and 14.77° in the out-of-plane profile, 13.22° and 14.77° in the in-plane profile; ODPA/DCHM: 13.74° and 15.09° in the out-of-plane profile, 13.60° and 14.86° in the in-plane profile), and the (004) peak was more distinctive compared with that of PMDA/DCHM (Table 2 and Figure 9a,b). Consequently, thermal treatment above T_g significantly enhances the packing order of PI chains, but it also causes isotropic orientation of the liquid-crystalline-like ordered domains.

The intensity of the amorphous halo increased in the order of PMDA/DCHM < BPDA/DCHM < ODPA/DCHM (Figure 9a,b), which indicates that the proportion of the amorphous matrix increases in this order. As mentioned above, the growth of ordered domains is prevented by bulky molecular structures, and the stacking between adjacent dianhydride moieties in Al-PIs leads to the ordered chain packing. Hence, the growth of the ordered domains should be remarkably influenced by the molecular structure of dianhydride. Figure 11 depicts the optimized molecular structures of one repeating unit of Al-PIs obtained by DFT calculations. BPDA has a rodlike but nonplanar structure, in which the torsion angle between two benzene rings is 41°. Hence, BPDA has a more stereoscopic structure than PMDA. In the case of ODPA, it possesses a bent molecular structure kinked at the diphenyl ether linkage, which results in the most stereoscopic structure among the dianhydrides (PMDA, BPDA, and ODPA). Accordingly, the difference in the proportion of the amorphous matrix is explainable by the

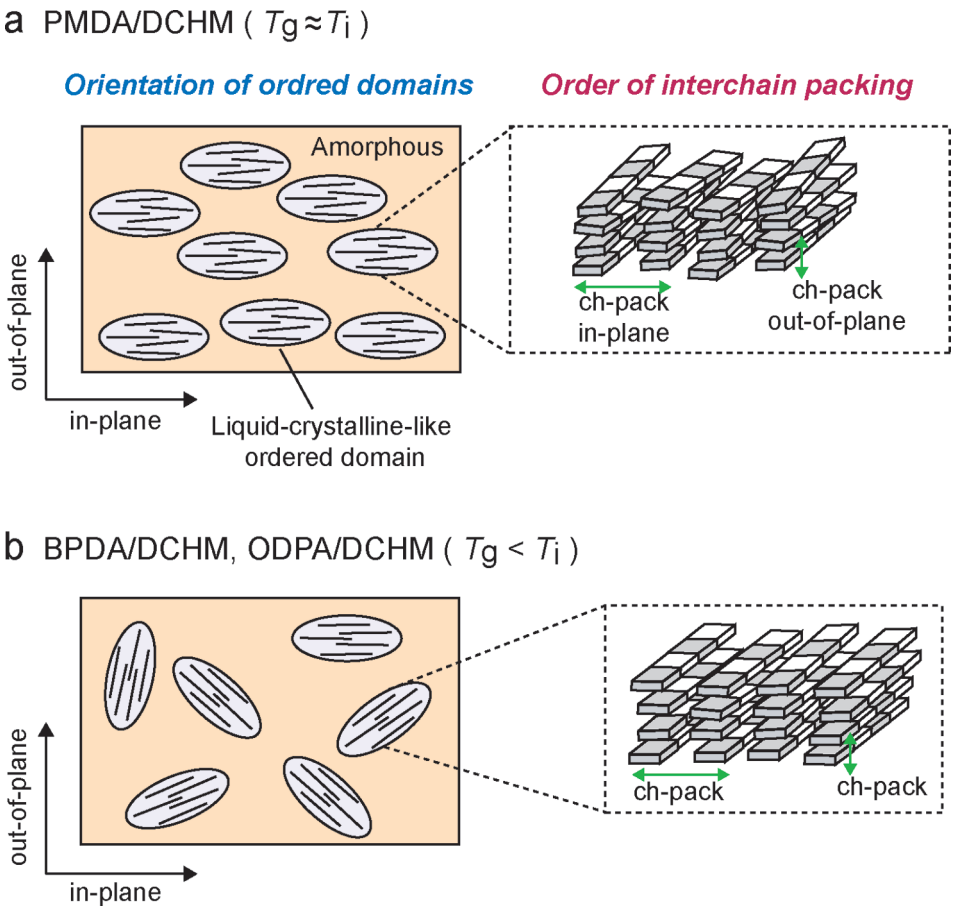

Figure 12. Schematic illustration of aggregation structure of (a) PMDA/DCHM and (b) BPDA/DCHM and ODPA/DCHM. Lines correspond to the PI chains, and circles denote the liquid-crystalline-like ordered domains. T_g and T_i denote the glass transition and imidization temperature, respectively.

three-dimensional molecular structure of the dianhydride moiety.

The schematic illustrations of the aggregation structures of Al-PIs are depicted in Figure 12. The lines correspond to the PI chains, and circles denote the liquid-crystalline-like ordered domains. In the case of PMDA/DCHM (Figure 12a), the PI chains are packed along the normal to the film plane in the liquid-crystalline-like ordered domains whose directors are oriented in the film plane. On the other hand, in the cases of BPDA/DCHM and ODPA/DCHM (Figure 12b), the directors of the liquid-crystalline-like ordered domains are randomly oriented, though the π-stack and ch-pack structures are maintained in the domains. In addition, the interchain ordering in the ordered domains is higher than that of PMDA/DCHM due to the vigorous rearrangement of PI chains during thermal imidization above T_g. However, the proportion of the ordered domains is lower than that of PMDA/DCHM, which originates from the bulky and stereoscopic molecular structure of the dianhydride moieties.

In summary, both of the three-dimensional structures of PI chains and the molecular reorientation during thermal imidization impart remarkable influences on the resultant aggregation structures of PIs. The former factor is predominant for Ar-PIs because their T_gs are much higher than T_i, whereas both factors are comparable for Al-PIs because their T_gs are close to or lower than T_i.

4. Conclusion

The intermolecular aggregation structures in thin films of fully aromatic polyimides (Ar-PIs) derived from pyromillitic dianhydride (PMDA) and those of semialiphatic polyimides (Al-PIs) from 4,4′-diaminocyclohexylmethane (DCHM) films formed on Si substrates were extensively examined by the grazing incidence wide-angle X-ray scattering (GIWAXS) technique. The aggregation structures of all PIs were identified as a mixture of the amorphous matrix and the liquid-crystalline-like ordered domains. The following characteristic scatterings were observed: amorphous halo, packing of PI chains, $\pi-\pi$ stacking of imide and phenyl rings, and repeating periodicity along PI chains. In the case of Ar-PIs, PI chains were packed along the in-plane and out-of-plane directions in the ordered domains. The growth of the ordered domains was essentially influenced by the steric effects of the molecular structure of PI chains. PMDA/PDA exhibited the weakest amorphous halo, a sharp ch-pack peak, and several higher-order (00*l*) peaks, which indicates that a rodlike molecular structure with high planarity is required for a well-ordered packing structure. In contrast, PMDA/ODA exhibited a weak ch-pack peak overlapped with a strong and broad amorphous halo, and higher-order (00*l*) peaks were not observed, which indicates that a nonplanar and bent molecular structure increases the defects in interchain packing. Furthermore, PMDA/TFDB, having a rodlike molecular structure, exhibited significantly larger *d*(ch-pack) values than those of the other PMDA-PIs, and its amorphous halo was weaker than that of PMAD/ODA. The bulky $-CF_3$ groups of the diamine moiety apparently increase the interchain distances in the ordered domains, but they do not impart remarkable influences on the packing structures in the amorphous matrix.

Although Al-PIs possess bent molecular structures similar to PMDA/ODA, the degrees of interchain ordering of Al-PIs

are higher than those of Ar-PIs, and they increased in the order of PMDA/DCHM < BPDA/DCHM < ODPA/DCHM. However, the degree of orientation in the liquid-crystalline-like ordered domains decreased as follows: PMDA/DCHM > BPDA/DCHM > ODPA/DCHM. These results indicate that the vigorous translational motion and rearrangement of PI chains occurring during thermal treatment close to or above T_g significantly enhance the packing order of PI chains, but they also cause isotropic orientation of the liquid-crystalline-like ordered domains. In contrast, the proportion of the amorphous matrix increased as follows: PMDA/DCHM < BPDA/DCHM < ODPA/DCHM, which indicates that bent and nonplanar dianhydride structure increases the proportion of amorphous matrix. Consequently, the intermolecular steric effects induced by the three-dimensional structures of PI chains and the motion of PI chains during thermal imidization have crucial influences on the aggregation structure of PIs. In addition, these experimental findings indicate that the GIWAXS technique is beneficial for the characterization of the aggregation structure of PI films formed on flat substrates.

Acknowledgment. This work was financially supported by the Japan Society for the Promotion of Science (Core University Program at Tokyo Institute of Technology). We also thank Yecheol Rho and Byungcheol Ahn at Pohang University of Science and Technology for their support in GIWAXS measurement and helpful discussions. M. Ree appreciates the financial supports of KOSEF (NRL Program and Center for Electro-Photo Behaviors in Advanced Molecular Systems) and Korean Ministry of Education, Science & Technology (MEST) (BK21 Program and World Class University Program). The synchrotron X-ray scattering measurements were supported by MEST, POSCO and POSTECH Foundation.

References and Notes

(1) Sroog, C. E. *J. Polym. Sci., Macromol. Rev.* **1976**, *11*, 161–208.
(2) Reuter, H.; Franke, H.; Feger, C. *Appl. Opt.* **1988**, *27*, 4565–4571.
(3) Jin, Q.; Yamashita, T.; Horie, K.; Yokota, R.; Mita, I. *J. Polym. Sci., Part A* **1993**, *31*, 2345–2351.
(4) Hasegawa, M.; Shindo, Y.; Sugimura, T.; Ohshima, S.; Horie, K.; Kochi, M.; Yokota, R.; Mita, I. *J. Polym. Sci., Part B* **1993**, *31*, 1617–1625.
(5) Matsuura, T.; Ando, S.; Sasaki, S.; Yamamoto, F. *Macromolecules* **1994**, *27*, 6665–6670.
(6) Li, Q.; Horie, K.; Yokota, R. *J. Photopolym. Sci. Technol.* **1997**, *10*, 49–54.
(7) Lee, S. A.; Yamashita, T.; Horie, K. *J. Polym. Sci., Part B* **1998**, *36*, 1433–1442.
(8) Sato, M.; Nakamoto, Y.; Yonetake, K.; Kido, J. *Polym. J.* **2002**, *34*, 601–607.
(9) Hasegawa, M.; Koyanaka, M. *High Perform. Polym.* **2003**, *15*, 47–64.
(10) Terui, Y.; Ando, S. *J. Polym. Sci., Part B* **2004**, *42*, 2354–2366.
(11) Pottiger, M. T.; Coburn, J. C.; Edman, J. R. *J. Polym. Sci., Part B* **1994**, *32*, 825–837.
(12) Hasegawa, M.; Matano, T.; Shindo, Y.; Sugimura, T. *Macromolecules* **1996**, *29*, 7897–7909.
(13) Terui, Y.; Matsuda, S.; Ando, S. *J. Polym. Sci., Part B* **2005**, *43*, 2109–2120.
(14) Russell, T. P.; Gugger, H.; Swalen, J. D. *J. Polym. Sci. Polym., Phys. Ed.* **1983**, *21*, 1745–1756.
(15) Takahashi, N.; Yoon, D. Y.; Parrish, W. *Macromolecules* **1984**, *17*, 2583–2588.
(16) Jou, J. H.; Huang, P. T. *Macromolecules* **1991**, *24*, 3796–3803.
(17) O'Mahoney, C. A.; Williams, D. J.; Colquhoun, H. M.; Mayo, R.; Young, S. M.; Askari, A.; Kendrick, J.; Robson, E. *Macromolecules* **1991**, *24*, 6527–6530.
(18) Cheng, S. Z. D.; Arnold, F. E.; Zhang, A.; Hsu, S. L. C.; Harris, F. W. *Macromolecules* **1991**, *24*, 5856–5862.
(19) Kitano, Y.; Usami, I.; Obata, Y.; Okuyama, K.; Jinda, T. *Polymer* **1995**, *36*, 1123–1126.
(20) Obata, Y.; Okuyama, K.; Kurihara, S.; Kitano, Y.; Jinda, T. *Macromolecules* **1995**, *28*, 1547–1551.
(21) Ree, M.; Kim, K.; Woo, S. H.; Chang, H. *J. Appl. Phys.* **1997**, *81*, 698–708.
(22) Saraf, R. F. *Polym. Eng. Sci.* **1997**, *37*, 1195–1209.
(23) Pyo, S. M.; Kim, S. I.; Shin, T. J.; Park, Y. H.; Ree, M. *J. Polym. Sci., Part A* **1999**, *37*, 937–957.
(24) Shin, T. J.; Lee, B.; Youn, H. S.; Lee, K.-B.; Ree, M. *Langmuir* **2001**, *17*, 7842–7850.
(25) Hsiao, S. H.; Chen, Y. J. *Eur. Polym. J.* **2002**, *38*, 815–828.
(26) Shin, T. J.; Ree, M. *J. Phys. Chem. B* **2007**, *111*, 13894–13900.
(27) Lee, B.; Park, I.; Yoon, J.; Park, S.; Kim, J.; Kim, K.-W.; Chang, T.; Ree, M. *Macromolecules* **2005**, *38*, 4311–4323.
(28) Heo, K.; Yoon, J.; Jin, S.; Kim, J.; Kim, K.-W.; Shin, T. J.; Chung, B.; Chang, T.; Ree, M. *J. Appl. Crystallogr.* **2008**, *41*, 281–291.
(29) Yoon, J.; Jung, S. Y.; Ahn, B.; Heo, K.; Jin, S.; Iyoda, T.; Yoshida, H.; Ree, M. *J. Phys. Chem. B* **2008**, *112*, 8486–8495.
(30) Yoon, J.; Jin, S.; Ahn, B.; Rho, Y.; Hirai, T.; Maeda, R.; Hayakawa, T.; Kim, J.; Kim, K.-W.; Ree, M. *Macromolecules* **2008**, *41*, 8778–8784.
(31) Jin, S.; Yoon, J.; Heo, K.; Park, H.-W.; Shin, T. J.; Chang, T.; Ree, M. *J. Appl. Crystallogr.* **2007**, *40*, 950–958.
(32) Kim, Y.; Cook, S.; Tuladhar, S. M.; Choulis, S. A.; Nelson, J.; Durrant, J. R.; Bradley, D. D. C.; Giles, M.; McCulloch, I.; Ha, C.-S.; Ree, M. *Nat. Mater.* **2006**, *5*, 197–203.
(33) Bolognesi, A.; Botta, C.; Mercogliano, C.; Porzio, W.; Jukes, P. C.; Geoghegan, M.; Grell, M.; Durell, M.; Trolley, D.; Das, A.; Macdonald, J. E. *Polymer* **2004**, *45*, 4133–4138.
(34) Josephkline, R.; McGehee, M. D.; Toney, M. *Nat. Mater.* **2006**, *5*, 222–228.
(35) Joshi, S.; Grigorian, S.; Pietsch, U.; Pingel, P.; Zen, A.; Neher, D.; Scherf, U. *Macromolecules* **2008**, *41*, 6800–6808.
(36) Yakabe, H.; Tanaka, K.; Nagamura, T.; Sasaki, S.; Sakata, O.; Takahara, A.; Kajiyama, T. *Polym. Bull.* **2005**, *53*, 213–222.
(37) Kawana, S.; Durrell, M.; Lu, J.; Macdonald, J. E.; Grell, M.; Bradley, D. D. C.; Jukes, P. C.; Jones, R. A. L.; Bennett, S. L. *Polymer* **2002**, *43*, 1907–1913.
(38) Knaapila, M.; Kisko, K.; Lyons, B. P.; Stepanyan, R.; Foreman, J. P.; Seeck, O. H.; Vainio, U.; Palsson, L. O.; Serimaa, R.; Torkkeli, M.; Monkman, A. P. *J. Phys. Chem. B* **2004**, *108*, 10711–10720.
(39) Cheun, H.; Liu, X.; Himpsel, F. J.; Knaaplia, M.; Scherf, U.; Torkkeli, M.; Winokur, M. J. *Macromolecules* **2008**, *41*, 6463–6472.
(40) Jukes, P. C.; Das, A.; Durell, M.; Trolley, D.; Higgins, A. M.; Geoghegan, M.; Macdonald, J. E.; Jones, R. A. L.; Brown, S.; Thompson, P. *Macromolecules* **2005**, *38*, 2315–2320.
(41) Liang, Y.; Zheng, M.; Park, K. H.; Lee, H. S. *Polymer* **2008**, *49*, 1961–1967.
(42) Jeng, U.; Hsu, C. H.; Sheu, H. S.; Lee, H. Y.; Inigo, A. R.; Chiu, H. C.; Fann, W. S.; Chen, S. H.; Su, A. C.; Lin, T. L.; Peng, K. Y.; Chen, S. A. *Macromolecules* **2005**, *38*, 6566–6574.
(43) Olsen, B. D.; Alcazar, D.; Krikorian, V.; Toney, M. F.; Thomase, E. L.; Segalman, R. A. *Macromolecules* **2008**, *41*, 58–66.
(44) Factor, B. J.; Russell, T. P.; Toney, M. F. *Macromolecules* **1993**, *26*, 2847–2859.
(45) Toney, M.; Russell, T. P.; Logan, J. A.; Kikuchi, H.; Sands, J. M.; Kumar, S. *Nature* **1995**, *374*, 709–711.
(46) Saraf, R. F.; Dimitrakopoulos, C.; Toney, M. F.; Kowalczyk, S. P. *Langmuir* **1996**, *12*, 2802–2806.
(47) Hirosawa, I.; Sasaki, N.; Kimura, H. *Jpn. J. Appl. Phys.* **1999**, *38*, L583–585.
(48) Matsumoto, T. *High Perform. Polym.* **1999**, *11*, 367–377.
(49) Oishi, Y.; Ogasawara, K.; Hirahara, H.; Mori, K. *J. Photopolym. Sci. Technol.* **2001**, *14*, 37–40.
(50) Oishi, Y.; Kikuchi, N.; Mori, K.; Ando, S.; Maeda, K. *J. Photopolym. Sci. Technol.* **2002**, *15*, 213–214.
(51) Yazdi, M. H.; Lee-Sullivan, P. *J. Therm. Anal. Calorim.* **2009**, *96*, 7–14.
(52) Yoon, J.; Kim, K. W.; Kim, J.; Heo, K.; Jin, K. S.; Jin, S.; Shin, T. J.; Lee, B.; Rho, Y.; Ahn, B.; Ree, M. *Macromol. Res.* **2008**, *16*, 575–585.
(53) Lee, B.; Park, Y.-H.; Hwang, Y.-T.; Oh, W.; Yoon, J.; Ree, M. *Nat. Mater.* **2005**, *4*, 147–150.
(54) Lee, B.; Oh, W.; Hwang, Y.; Park, Y.-H.; Yoon, J.; Jin, K. S.; Heo, K.; Kim, J.; Kim, K.-W.; Ree, M. *Adv. Mater.* **2005**, *17*, 696–701.
(55) Lee, C.; Yang, W.; Parr, R. G. *Phys. Rev.* **1988**, *B37*, 785–789.
(56) Miehlich, B.; Savin, A.; Stoll, H.; Preuss, H. *Chem. Phys. Lett.* **1989**, *157*, 200–206.

(57) Becke, A. D. *J. Chem. Phys*. **1993**, *98*, 5648–5652.
(58) Frisch, M. J.; Trucks, G. W.; Schlegel, H. B.; Scuseria, G. E.; Robb, M. A.; Cheeseman, J. R.; Montgomery, Jr., J. A.; Vreven, T.; Kudin, K. N.; Burant, J. C.; Millam, J. M.; Iyengar, S. S.; Tomasi, J.; Barone, V.; Mennucci, B.; Cossi, M.; Scalmani, G.; Rega, N.; Petersson, G. A.; Nakatsuji, H.; Hada, M.; Ehara, M.; Toyota, K.; Fukuda, R.; Hasegawa, J.; Ishida, M.; Nakajima, T.; Honda, Y.; Kitao, O.; Nakai, H.; Klene, M.; Li, X.; Knox,J. E.; Hratchian, H. P.; Cross, J. B.; Bakken, V.; Adamo, C.; Jaramillo, J.; Gomperts, R.; Stratmann, R. E.; Yazyev, O.; Austin, A. J.; Cammi, R.; Pomelli, C.; Ochterski, J. W.; Ayala, P. Y.; Morokuma, K.; Voth, G. A.; Salvador, P.; Dannenberg, J. J.; Zakrzewski, V. G.; Dapprich, S.; Daniels, A. D.; Strain, M. C.; Farkas,O.; Malick, D. K.; Rabuck, A. D.; Raghavachari, K.; Foresman, J. B.; Ortiz, J. V.; Cui, Q.; Baboul, A. G.; Clifford, S.; Cioslowski, J.; Stefanov, B. B.; Liu,G.; Liashenko,A.; Piskorz, P.; Komaromi,I.; Martin, R. L.; Fox, D. J.; Keith, T.; Al-Laham, M. A.; Peng, C. Y.; Challacombe, A. M.; Gill, P. M. W.; Johnson, B.; Chen, W.; Wong, M. W.; Gonzalez, C.; Pople, J. A. *Gaussian 03, Revision D.02*; Gaussian, Inc.: Wallingford, CT, 2004.
(59) Yoon, J.; Jin, K. S.; Kim, H. C.; Kim, G.; Heo, K.; Jin, S.; Kim, J.; Kim, K.-W.; Ree, M. *J. Appl. Crystallogr*. **2007**, *40*, 476–488.
(60) Asano, T.; Baltá Callejá, F. L.; Flores, A.; Tanigaki, M.; Mina, M. F.; Sawatari, C.; Itagaki, H.; Takahashi, H.; Katta, I. *Polymer* **1999**, *40*, 6475–6484.